

# Orientation of Phenyl Rings and Methylene Bisectors at the Free Surface of Atactic Polystyrene

Thomas C. Clancy, Jee Hwan Jang, Ali Dhinojwala, and Wayne L. Mattice\*

*Institute of Polymer Science, The University of Akron, Akron, Ohio 44325-3909*

*Received: April 26, 2001; In Final Form: September 6, 2001*

Atomistically detailed models of free-standing thin films and the bulk structure of amorphous atactic polystyrene have been produced by reverse mapping from equilibrated coarse-grained models. The bridging technique employed in the simulation allows the generation of a moderate sized atomistic system (six independent parent chains of  $C_{400}H_{402}$ , 4812 atoms) with a more reasonable computational effort than is required when all of the construction is performed on chains expressed with atomistic detail. Reverse mapping from the coarse-grained model to the atomistically detailed model is found to be straightforward, without ring piercing or concatenation. The calculated surface energy ( $38 \pm 10$  erg/cm<sup>2</sup>) is in reasonable agreement with prior experimental findings. The surface of the thin films is enriched in phenyl rings. The rings at the surface tend to be oriented so that they are pointing outward, but rings in the middle of the thin film show no preferred orientation. In contrast with the phenyl rings, the bisectors for the methylene groups show little tendency for orientation, even when the methylene groups are close to the surface. These observations in the simulation are in qualitative agreement with conclusions reported recently (Gautam et al. *Phys. Rev. Lett.* **2000**, *30*, 3854, and Briggman et al. *J. Phys. Chem. B* **2001**, *105*, 2785), based on the application of new spectroscopic techniques to the characterization of polymer surfaces.

## Introduction

The importance of polymer surfaces in numerous applications has prompted the recent development of new experimental techniques for their characterization. One of the important issues is the local structure, which can be expressed in terms of preferences for orientation of various groups when such groups are located close to a surface. Recently a new experimental technique, IR–visible sum–frequency spectroscopy with total internal reflection geometry, has detected an interesting orientation pattern at the free surface of atactic polystyrene.<sup>1</sup> This technique finds a strong tendency for orientation of the phenyl side chains, with the *c*-axis of the phenyl group (defined by the ring carbon atom bonded to the backbone and the ring carbon atom in the para position) tending to be aligned with the surface normal. However, the same technique finds little tendency for the orientation of the methylene groups. Similar behavior of the phenyl groups was reported subsequently by another group.<sup>2</sup> The present work describes an atomistically detailed model for a free-standing thin film of atactic polystyrene, generated by a new simulation technique. The surface structure in the model confirms, and extends, the major features reported in the experiments.<sup>1,2</sup>

The free-standing thin film is generated from a model for the bulk polymer, using a technique that involves a large change in the periodic boundary in one direction, followed by a reequilibration of the model.<sup>3</sup> This technique has been employed previously for the construction of free-standing thin films using atomistically detailed models of several polymeric hydrocarbons<sup>4–6</sup> and coarse-grained models of polyethylene.<sup>7</sup> The use of coarse-grained models permits the construction of more thoroughly equilibrated, and larger, models than is possible using the atomistically detailed representation of the system.

Bulk amorphous polystyrene has been the subject of several prior studies that employed fully atomistic detail<sup>8–11</sup> or a united atom description of the chain.<sup>10</sup> Roe's united atom model used five sites for each monomer unit.<sup>10</sup> Our more coarsely grained model uses only a single site for each monomer unit. The single site is located at the position of the carbon atom in the main chain to which the side chain is attached. This level of coarse-graining has been successfully applied to simulations of polypropylene melts.<sup>12</sup> It successfully reproduces the known dependence of the miscibility of these melts on the stereochemical composition of the chains,<sup>13–16</sup> and also provides the mechanism responsible for the demixing of syndiotactic polypropylene from either isotactic or atactic polypropylenes in the melt.<sup>12</sup> Therefore our treatment of coarse-grained chains can successfully mimic subtle interactions in multichain systems. This simulation method, as applied to polyethylene melts, has been reviewed recently.<sup>17,18</sup>

## Method

For both the thin film and the amorphous cell, six atactic chains of 50 monomer units ( $H(CH(C_6H_5)CH_2)_{50}H$ ) were simulated. The coarse-grained 2nnd lattice method was applied in the same manner as done previously for polypropylene<sup>12,19</sup> and poly(vinyl chloride).<sup>20</sup> The local intrachain interactions were controlled by the rotational isomeric state model described by Yoon et al.<sup>21</sup> for polystyrene, which was mapped onto the coarse-grained chains on a high coordination lattice. The high coordination lattice has  $10i^2 + 2$  sites in shell *i*, and a step length of 2.50 Å. This procedure causes the coarse-grained chains, and their component subchains, to prefer the proper distribution of end-to-end distances for unperturbed polystyrenes of the specified stereochemical sequence. The intermolecular interactions are introduced by discretization of a continuous potential energy function, using the method introduced by Cho.<sup>22</sup>

\* Author to whom correspondence should be addressed.

**TABLE 1: Shell Energies (kJ/mol) Derived from L-J Parameters for Four Small Molecules**

monomer	ethane	propane	ethyl chloride	toluene
$\epsilon/k_B$ (K)	205.0	237.1	300.0	377.0
$\sigma$ (Å)	4.4	5.118	4.898	5.932
$T$ (K)	443	473	450	600
1st shell	14.215	26.851	21.968	86.4
2nd shell	0.429	3.068	1.575	11.53
3rd shell	-0.698	-1.089	-1.369	-1.15
4th shell	-0.172	-0.464	-0.468	-1.46
5th shell	-0.045	-0.127	-0.124	-0.48

The coarse-grained models are simulated by a dynamic Monte Carlo algorithm at 600 K in order to effectively move the chains during the course of the simulation. Snapshots of the trajectory are taken and low energy conformations are chosen for reverse-mapping. Each configuration that is reverse-mapped is a statistically distinct conformation as indicated by the average displacement of the center of mass of a chain with respect to the mean square radius of gyration and the decay of the autocorrelation function of the end-to-end vector. Initially, the reverse-mapped models are energy minimized using the same procedure that was used for the polyethylene reverse-mapping.<sup>23</sup> Due to the presence of the bulky phenyl side groups, a short (100 ps) MD trajectory was applied to these initially minimized structures. Snapshots of this MD trajectory were taken and the one with the lowest potential energy was selected for the final energy minimization. For the thin film simulation, *NVT* dynamics at 298 K was applied. For the amorphous cell simulation *NpT* dynamics at 298 K and  $p = 0.15$  GPa was applied for 50 ps followed by *NpT* dynamics at 298 K and  $p = 0.25$  GPa. The model was then compressed to achieve the correct density.

**Short-Range Energy.** A rotational isomeric state model of polystyrene<sup>21</sup> was applied to the short-range interaction of beads along the chain with values of the energies of the short-range intramolecular interactions assigned as  $E_\eta = -1.7$ ,  $E_\omega = 8.4$ ,  $E_{\omega X} = 8.4$ , and  $E_{\omega XX} = 9.2$  kJ/mol, along with preexponential factors of 0.8 for  $\eta$ , 1 for  $\omega$ , and 1.3 for  $\omega X$  and  $\omega XX$ . In order for the MC algorithm to function properly, it was necessary to apply a large but finite (50 kJ/mol) energy for the  $\tau$  interaction. This energy was taken to be infinite in the rotational isomeric state model of Yoon et al.<sup>21</sup> In the present simulation, the value is chosen to be high enough so that the time-averaged population of this conformation is negligible, but the value is also low enough so that this conformation is accessible as a transition state in order to allow the MC dynamics to proceed on a reasonable time scale.

**Long-Range Energy.** The long-range interaction for styrene monomers in their coarse-grained representation on the discrete space of the high coordination lattice was calculated using the method of Cho and Mattice.<sup>22</sup> The Lennard-Jones (L-J) values tabulated<sup>24</sup> for toluene were used to estimate this interaction. Values for ethylbenzene, which would be a more appropriate molecule, were not found in the reference used. However, considering the range of experimentally derived values that are tabulated for any given compound, this would not seem to be significant, given our current method for estimating long-range energies. Table 1 shows the energy values for each shell on the high coordination lattice, as calculated for toluene. For comparison, values for ethane, propane, and ethyl chloride, which have been used as input for similar simulations of polyethylene, polypropylene, and poly(vinyl chloride), are also shown. Due to the larger value of  $\sigma$  for the L-J interaction of toluene, the minimum in the discretized shell energies is in the fourth shell for toluene, whereas it was in the third shell for the three smaller molecules.

A perturbation for the interaction in the 2nd shell was estimated as was done previously for polypropylene.<sup>19</sup> Normalizing over all 672 ( $= 4 \times 4 \times 42$ ) orientations on the high coordination lattice yields a perturbation which lowers the energy of the 2nd shell by  $\sim 13.19$  kJ/mol in the case where the phenyl rings are pointing away from each other and increases the energy by  $\sim 37.96$  kJ/mol when the rings are pointed directly at each other. To invoke a neutral interaction for the former case, the perturbation is scaled by a factor of 0.87. This should be a reasonably accurate estimate for the case where the two phenyl rings are pointing away from each other since the interaction for polyethylene is close to 0 for the 2nd shell interactions, as shown in Table 1. It is probably an underestimate for the case where the two phenyl rings are pointed directly at each other, since they would probably be overlapping in this case. However, the desired goal is achieved in that no case of ring concatenation or ring spearing is seen in the reverse-mapped replicas.

**Thin Films.** Models of thin films were developed as done previously in similar simulations of polyethylene.<sup>7</sup> One of the coordinates of the periodic box was extended (forty 2nd lattice units) to effectively produce periodic boundary conditions in two dimensions, rather than the three dimensions used for the original amorphous cell. It was necessary to employ four shells in the long range energy evaluation in order to maintain a cohesive thin film at the proper density. Using only three shells in the long range energy caused the film to spread out and uniformly fill the extended periodic boundary cell at a much lower density. Prior 2nd simulations of polyethylene,<sup>7,22,23</sup> polypropylene,<sup>12</sup> and poly(vinyl chloride)<sup>20</sup> often retained only 3 shells for the intermolecular interaction, but in these previous simulations the discretized L-J potential had its minimum in the third shell, while the minimum moves to the fourth shell in the present simulation of polystyrene, as shown in Table 1. Five representative snapshots of the 2nd trajectory ( $1 \times 10^7$  Monte Carlo steps) were subject to the reverse-mapping procedure. These reverse-mapped models were then equilibrated with a short (100 ps) MD run, followed by a final energy minimization using the pcff force field from Molecular Simulations, Inc. This last step causes the atomistically detailed model to fall into a local conformational energy minimum in continuous space, located close to the site in discrete configuration space produced by the prior Monte Carlo simulation with the coarse grained model. The final result is more strongly influenced by the parameters employed in the extensive Monte Carlo simulation than by the force field adopted for the subsequent short MD run. The average density of the thin films was found to be 1.0985 g/cm<sup>3</sup> in the middle (bulk) section of the thin films. This value was used in the bulk amorphous cell simulation in order to match the density of the interior of the thin films with that of the bulk model.

**Bulk Amorphous Cells.** The coarse-grained polystyrene model was run on the 2nd lattice for  $1 \times 10^7$  Monte Carlo steps at a density of 1.1469 g/cm<sup>3</sup>. Upon reverse mapping, the density is adjusted by increasing the length of the periodic box from 40.000 to 40.578 Å, to produce the desired density for the amorphous cell that is used as the reference in the computation of the surface energy.

## Results and Discussion

**Pair Correlation Functions in the Amorphous Cells.** Intermolecular pair correlation functions for the carbon atoms in the amorphous bulk cells are depicted in Figure 1. As expected, there is closer packing of the carbon atoms in the

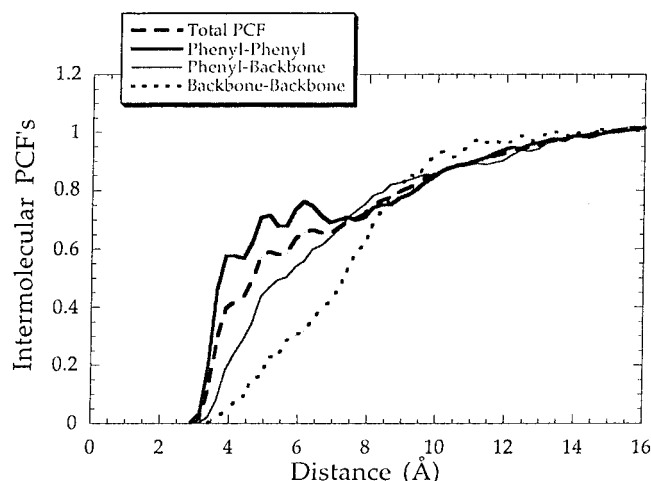


**Figure 1.** Intermolecular pair correlation functions for the carbon atoms in the amorphous cells of atactic polystyrene. All carbon atoms, dashed line. Ring–ring pair correlation function, thick solid line. Backbone–backbone pair correlation function, dotted line. Backbone–ring pair correlation function, thin solid line.

**TABLE 2: Energetic Analysis**

	energy of thin films (kJ/mol)	energy of amorphous cells (kJ/mol)	surface tension (erg/cm <sup>2</sup> )
total	−840 ± 33	−991 ± 21	38 ± 10
bonded portion	−1133 ± 24	−930 ± 20	−51 ± 8
nonbonded portion	294 ± 32	−61 ± 9	89 ± 8

phenyl rings than in the packing of the carbon atoms in the backbone. The phenyl–phenyl intermolecular pair correlation in Figure 1 is similar to the one reported by Khare et al.,<sup>8</sup> rising sharply from nearly 0 at 3 Å to a value of about 0.6 at 4 Å, and then increasing gradually, reaching a value of about 0.9 at the largest distance (12 Å) reported by Khare et al. The increase in the backbone–ring and backbone–backbone intermolecular pair correlation functions is more gradual and occurs at somewhat larger distance, reaching a value of 0.5 at a distance of about 6 Å (backbone–ring) and just above 7 Å (backbone–backbone) both in Figure 1 and in Khare et al.<sup>8</sup>

**Energies.** The average energies of the five amorphous cells and thin films are shown in Table 2. The total energy can be decomposed into a bonded portion and a nonbonded portion. The bonded portion consists of energetic terms associated with chemically bonded atoms, such as torsions, angle bending, bond stretching, and cross terms of these. The nonbonded portion consists of the van der Waals and electrostatic contributions. The surface tension is calculated from eq 1:

$$\gamma = (E_{\text{thin film}} - E_{\text{amorphous cell}})/2A \quad (1)$$

Here  $E_{\text{thin film}}$  is the average energy the thin films,  $E_{\text{amorphous cell}}$  is the average energy of the bulk amorphous cells, and  $A$  is the area exposed on one of the two newly created surfaces. The average surface tension agrees reasonably well with experimental measurements (39.3–40.7 erg/cm<sup>2</sup>) for polystyrene at 293 K.<sup>25</sup> The surface tension consists of a positive contribution from the nonbonded interaction and a negative contribution from the bonded portion. This behavior was seen in previous simulations of simpler polymeric hydrocarbons.<sup>3–6</sup> It indicates a relaxation of the intramolecular conformational energy in the low density environment near the surface, which partially offsets the increase in energy due to the sacrifice in potentially attractive nonbonded interactions. The large uncertainty in the calculated

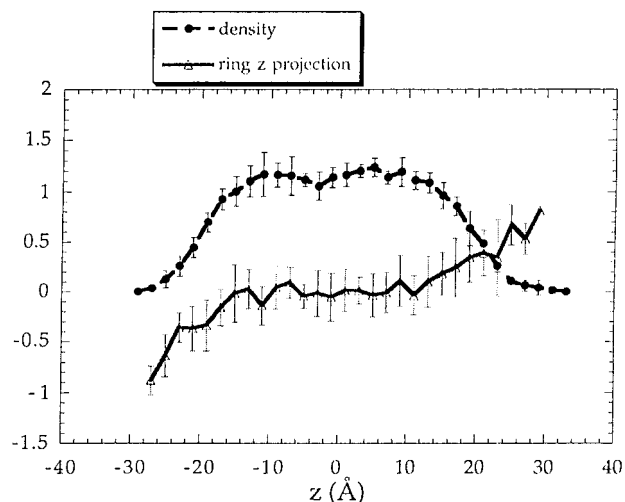


**Figure 2.** The density profile (g/cm<sup>3</sup>) normal to the surface of the film is presented by the filled circles. The horizontal axis originates at the midpoint of the thin film. Open triangles depict the order parameter for the phenyl side chains.

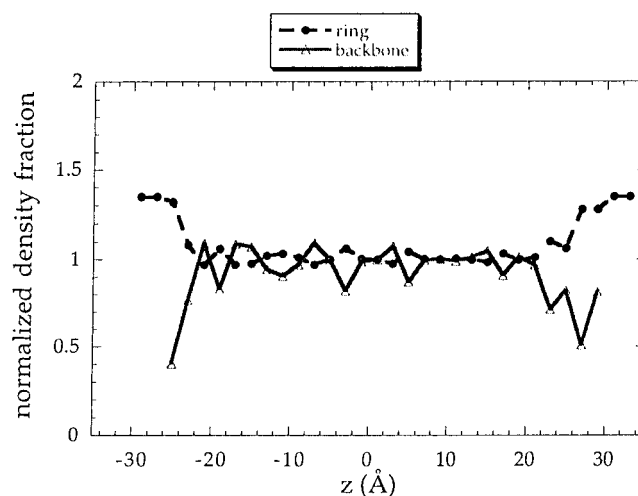


**Figure 3.** Normalized density profiles for the C<sub>6</sub>H<sub>5</sub> units (filled circles connected by dashed line) and CHCH<sub>2</sub> backbone (open triangles connected by solid line) in the thin films.

surface energy is typical of simulations performed with this technique<sup>3–6</sup> and also with simulation using a very different technique.<sup>26</sup>

**Density Profiles.** The filled symbols in Figure 2 depict the density profiles along the  $z$ -axis, which is normal to the surface. The position  $z = 0$  is located in the middle of the thin film. The density profiles are averaged over the five independent reverse-mapped snapshots. A density slight larger than 1 g/cm<sup>3</sup> is obtained at the plateau region in the interior of the film. At either surface, the density decays from the plateau value to zero over a distance on the order of 10 Å, which is typical for simulations of the surfaces of polymeric hydrocarbons.<sup>3–6,26</sup>

Figure 3 depicts the normalized density profiles for the phenyl groups (C<sub>6</sub>H<sub>5</sub>) and for the backbone (CHCH<sub>2</sub>). The normalization will produce a value of 1 if the relative population of the groups in each bin is the result expected from the composition of the repeat unit. Values not distinguished from 1 are obtained in the dense interior of the thin films. However, in those regions where the overall density (Figure 2) is low, there is a tendency in Figure 3 for the rings to contribute a normalized density larger than 1, and a corresponding tendency for the backbone to contribute a normalized density less than 1. This result shows



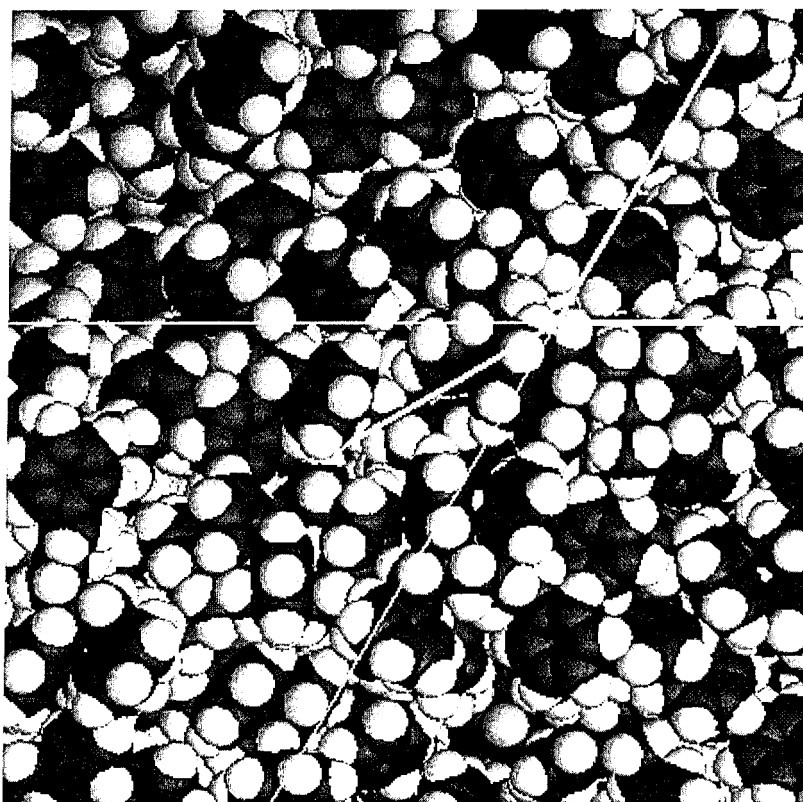


**Figure 4.** Snapshot of the surface, viewed along the  $z$ -axis from outside the film. The straight lines are outlines of the edges of the periodic cell used in the simulation.

that the low-density surface region is enriched in phenyl rings. This observation in the simulation is consistent with the conclusions from experiments.<sup>1,2</sup>

**Orientation of the Phenyl Rings.** The orientation of the phenyl rings is evaluated using the angle,  $\theta$ , between the  $z$ -axis and a vector in the ring that points from the carbon atom that is bonded to the backbone to the carbon atom in the para position. The location of the midpoint of this vector is used for assigning the orientation values of bins in the  $z$ -direction. The order parameter,  $\langle \cos \theta \rangle$ , is 1 if this vector points in the positive  $z$ -direction,  $-1$  if it points in the negative  $z$ -direction, and zero for no preferred orientation. The results from the simulation are presented with the open symbols in Figure 2. The order parameter is not distinguishable from zero in that portion of the film in which the density has achieved its plateau value. In the surface region, where the density is lower and there is an excess of phenyl groups (Figure 3), the order parameter is distinguishable from 0, and approaches values near  $\pm 1$ . The signs of the nonzero order parameters in these two surface regions show that the phenyl rings tend to point outward, away from the surface.

Recent spectroscopic experiments show that the  $c$ -axis of the phenyl groups at the surface tends to be nearly aligned with the surface normal,<sup>1,2</sup> which is qualitatively consistent with the result depicted in Figure 2. Gautam et al.<sup>1</sup> suggest that the representative value of  $\theta$  is about  $20^\circ$ , which corresponds to an absolute value of about 0.94 for the order parameter used in Figure 2. Briggman et al.<sup>2</sup> report a somewhat weaker tendency for orientation, with  $\theta$  in the range  $49^\circ$ – $65^\circ$ , corresponding to an order parameter with an absolute value of 0.42–0.65. Quantitative agreement between simulation and either experiment demands that the experiments probe the orientation of only those  $C_6H_5$  groups at the extreme outer limit of the surface, where the density has fallen to no more than half of its bulk

value. Furthermore, the simulation suggests that the average value of  $\theta$  sensed in an experiment will be extremely sensitive to its depth of penetration into the film.

Gautam et al.<sup>1</sup> could not resolve the direction of the orientation of the phenyl groups in the surface region, but Briggman et al.<sup>2</sup> report that the direction has the phenyl groups pointing outward, away from the interior of the film. The sign of the order parameter in Figure 2 shows that the direction of orientation is indeed outward.

A snapshot of one of the surfaces, view along the  $z$ -axis from outside the film, is depicted in Figure 4. Casual inspection quickly reveals the faces of a few rings that tend to be oriented perpendicular to the surface. Closer inspection detects the edges of a larger number of rings that tend to be sticking out of the film, toward the viewer. It is this latter group of rings that dominates the behavior of the order parameter in the surface region.

**Orientation of the Methylene Units.** The orientation of the methylene units is determined with its bisector, defined as the sum of the two C–H vectors that originate at the carbon atom and terminate at a hydrogen atom. Here  $\theta$  is defined as the angle between the bisector and the  $z$ -axis. The value of  $\langle \cos \theta \rangle$  for this bisector is depicted in Figure 5. There is no convincing evidence for preferred orientation of the methylene groups in any portion of the thin film. This conclusion from the simulation is consistent with the deduction from the experiments of Gautam et al.<sup>1</sup>

**Rationalization of the Differences in the Orientation of the Rings and Methylene Groups.** A very simple model can rationalize the absence of significant orientation of the methylene groups, even when the rings are strongly oriented. For this purpose we use the *mm*, *mr*, and *rr* stereoisomers of 2,4,6-triphenylheptane as models for the isotactic, heterotactic, and syndiotactic triads of polystyrene. A  $Z$ -axis is defined by the

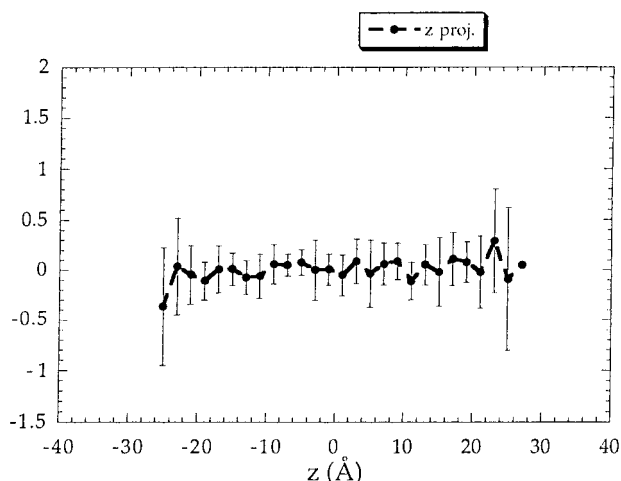


**Figure 5.** Order parameter for the bisector of the methylene groups in the thin films.

**TABLE 3: Analysis of the Stereoisomers of 2,4,6-Triphenylheptane**

configuration	preferred conformation(s)	angles <sup>a</sup>
<i>mm</i>	<i>tggt</i> (or <i>gtgt</i> )	0° and 120°
<i>mr</i>	<i>tggt</i>	0° and 120°
<i>mr</i>	<i>gttt</i>	both 120°
<i>rm</i>	<i>ttgt</i>	0° and 120°
<i>rm</i>	<i>tttg</i>	both 120°
<i>rr</i>	<i>tttt</i>	both 120°

<sup>a</sup> Angle between the Z-axis defined in the text and the bisectors of the methylene groups at positions 3 and 5.

phenyl group bonded to carbon 4, with this axis pointing from the ring carbon atom bonded to the backbone to the ring carbon atom in the para position. By definition, this ring has an order parameter of 1.

The order parameters for the bisectors of the methylene groups on either side of this ring, i.e., the bisectors of the methylene groups at carbon atoms 3 and 5 of the heptane backbone, are determined using the preferred conformations of the triads in polystyrene. The meso diads prefer *tg* or *gt* conformations, and the racemo diad prefers the *tt* conformation. The preferred conformations of the internal C–C bonds in the heptane backbone are therefore the ones presented in Table 3. This table also presents the angles between the Z-axis defined in the previous paragraph and the bisectors of the methylene groups at carbon atoms 3 and 5, using these preferred conformations and internal torsion angles of 180° for *t* and  $\pm 60^\circ$  for the *g* conformations. If we assume the triads in atactic polystyrene occur in the ratio 1:1:1:1 for *tt*, *mr*, *rm*, and *rr*, and further assume that the *tggt* and *gttt* conformations are equally probable for *mr*, and the *ttgt* and *tttg* conformations are equally probable for *rm*, then  $\langle \cos \theta \rangle = -1/8$ . According to this very simple model, the highest possible ordering of the central phenyl ring would be accompanied by only a weak ordering of the bisectors of its neighboring methylene groups.

## Conclusion

Applying a reverse-mapping procedure to a coarse-grained model allows the generation of atomistic models of thin films

of atactic polystyrene. The surface tension yields reasonable values as compared with experiment and the density of the thin films of the reverse-mapped structures is reasonable. There is no detectable preference in the orientation of the methylene groups. The phenyl groups are enriched at the surface, and the phenyl groups in the surface regions tend to have their *c*-axis aligned with the normal to the surface of the film. These orientational properties are consistent with conclusions from a recent experimental study by Gautam et al.<sup>1</sup> and Briggman et al.<sup>2</sup> The simulation also establishes that the phenyl rings in the surface region point outward, as reported by Briggman et al.<sup>2</sup> The experimental assessment of the strength of the orientation of the phenyl groups will be extremely sensitive to the depth of penetration of that experiment into the thin film. Bisectors for the methylene groups experience little order anywhere in the film.

**Acknowledgment.** This work was supported by National Science Foundation Grant DMR 0098321.

## References and Notes

- (1) Gautam, K. S.; Schwab, A. D.; Dhinojwala, A.; Zhang, D.; Dougal, S. M.; Yeganeh, M. S. *Phys. Rev. Lett.* **2000**, *30*, 3854.
- (2) Briggmann, K. A.; Stephenson, J. C.; Wallace, W. E.; Richter, L. J. *J. Phys. Chem. B* **2001**, *105*, 2785.
- (3) Misra, S.; Fleming, P. D.; Mattice, W. L. *J. Comput.-Aided Mater. Des.* **1995**, *2*, 101.
- (4) Natarajan, U.; Tanaka, G.; Mattice, W. L. *J. Comput.-Aided Mater. Des.* **1997**, *4*, 193.
- (5) Natarajan, U.; Misra, S.; Mattice, W. L. *Comput. Theor. Polym. Sci.* **1998**, *8*, 323.
- (6) Clancy, T. C.; Mattice, W. L. *Comput. Theor. Polym. Sci.* **1999**, *9*, 261.
- (7) Doruker, P.; Mattice, W. L. *Macromolecules* **1998**, *31*, 1418.
- (8) Khare, R.; Paulaitis, M. E.; Lustig, S. R. *Macromolecules* **1993**, *26*, 7203.
- (9) Rapold, R. F.; Suter, U. W.; Theodorou, D. N. *Macromol. Theory Simul.* **1994**, *3*, 19.
- (10) Mondello, M.; Yang, H.-J.; Furuya, H.; Roe, R.-J. *Macromolecules* **1994**, *27*, 3566.
- (11) Ayyagari, C.; Bedrov, D.; Smith, G. D. *Macromolecules* **2000**, *33*, 6194.
- (12) Clancy, T. C.; Pütz, M.; Weinhold, J. D.; Curro, J. G.; Mattice, W. L. *Macromolecules* **2000**, *33*, 9352.
- (13) Lohse, D. *Polym. Eng. Sci.* **1986**, *26*, 1500.
- (14) Thomann, R.; Kressler, J.; Setz, S.; Wang, C.; Mülhaupt, R. *Polymer* **1996**, *37*, 2627.
- (15) Thomann, T.; Kressler, J.; Rudolf, B.; Mülhaupt, R. *Polymer* **1996**, *37*, 2635.
- (16) Maier, R. D.; Thomann, R.; Kressler, J.; Mülhaupt, R.; Rudolf, B. *J. Polym. Sci., Part B* **1997**, *35*, 1135.
- (17) Doruker, P.; Mattice, W. L. *Macromol. Theory Simul.* **1999**, *8*, 463.
- (18) Baschnagel, J.; Binder, K.; Doruker, P.; Gusev, A. A.; Hahn, O.; Kremer, K.; Mattice, W. L.; Müller-Plathe, F.; Murat, M.; Paul, W.; Santos, S.; Suter, U. W.; Tries, V. *Adv. Polym. Sci.* **2000**, *152*, 41.
- (19) Clancy, T. C.; Mattice, W. L. *J. Chem. Phys.* **2000**, *112*, 10049.
- (20) Clancy, T. C.; Mattice, W. L. *Macromolecules* **2001**, *34*, 6482.
- (21) Yoon, D. Y.; Sundararajan, P. R.; Flory, P. J. *Macromolecules* **1975**, *8*, 776.
- (22) Cho, J.; Mattice, W. L. *Macromolecules* **1997**, *30*, 637.
- (23) Doruker, P.; Mattice, W. L. *Macromolecules* **1997**, *30*, 5520.
- (24) Reid, R. C.; Prausnitz, J. M.; Poling, B. E. *The Properties of Gases and Liquids*, 4th ed.; McGraw-Hill: New York, 1987.
- (25) Brandup, J.; Immergut, E. H.; Grulke, E. A.; Abe, A.; Block, D. R. *Polymer Handbook*, 4th ed.; John Wiley & Sons: New York, 1999.
- (26) Mansfield, K. F.; Theodorou, D. N. *Macromolecules* **1990**, *23*, 4430.